A Temperature Controller IC for Maximizing Si Micro-Ring Modulator Optical Modulation Amplitude

Min-Hyeong Kim, *Student Member, IEEE*, Lars Zimmermann, and Woo-Young Choi, *Member, IEEE*

***Abstract*—We present a custom-designed integrated circuit (IC) implemented in 0.25-μm BiCMOS technology that can automatically control the Si micro-ring modulator (MRM) temperature for optimal modulation characteristics. The IC monitors the optical modulation amplitude (OMA) of an Si MRM and provides the optimal heater setting for the maximum OMA. The IC consists of trans-impedance amplifier, power detector, track-and-hold circuit, comparator, digital-to-analog converter, and digital controller, all of which are integrated in a single chip. We demonstrate that, with this IC, an Si MRM can provide the maximum OMA for 25-Gb/s operation despite changes in temperature and input optical power.**

***Index Terms*—Digital control circuit, integrated circuit (IC), monolithic integration, optical modulation amplitude (OMA), Si micro-ring modulator (Si MRM), Si photonics, temperature control, wavelength locking.**

I. Introduction

With the explosive wireless and wireline data traffic increase, there is a great demand for high-performance interconnects for building-to-building, floor-to-floor, rack-to-rack, and board-to-board applications. Since it is becoming difficult to satisfy the increasingly demanding interconnect requirements with the conventional electrical interconnects, there is a great amount of research effort for realizing interconnect solutions based on photonics. In particular, Si photonics attracts lots of attention since it promises realization of high-performance optical interconnect solutions with the cost-effective mass-production capability [1].

Among many Si photonic devices, the modulator is arguably the most important device as Si photonics technology cannot provide reliable and efficient light sources that can be realized with the standard Si processing technology. Although the Si Mach-Zehnder modulator (MZM) is widely used for many Si photonics applications, its footprints are too large for future inter-chip and intra-chip optical interconnect applications where the size of interconnect solutions is an important factor. Consequently, the Si micro-ring modulator (MRM) receives special research interests as it can provide high-bandwidth interconnect solutions with the advantages of small footprints and the resulting small electrical loads [2]. However, with its resonance characteristics, it suffers from the critical thermal sensitivity problems.

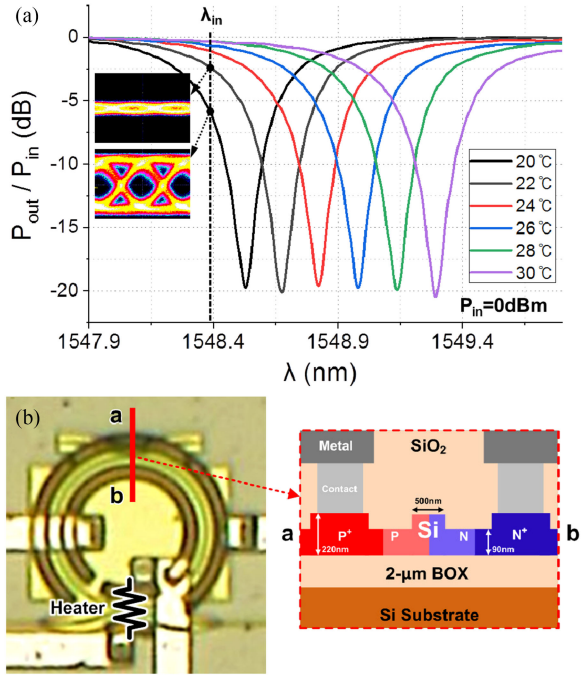

Fig. 1. (a) Normalized transmission spectra of sample Si MRM at six different temperatures and eye diagrams at temperatures of two-degree difference and (b) microphotograph of the sample Si MRM with its cross-sectional diagram.

The Si MRM resonance wavelength has strong dependence on temperature. Fig. 1(a) shows the temperature dependence of measured transmission characteristics for a sample Si MRM at six different temperatures ranging from 20 °C to 30 °C with 0-dBm input optical power. Measured eye diagrams are also shown when the device is modulated with 25-Gbps data at temperatures of two-degree difference with the same input light wavelength (λ_{in}). As shown in the figure, the eye opening can disappear completely with only two-degree change in temperature. For the measurement, a depletion-type Si MRM having

Manuscript received July 25, 2018; revised October 3, 2018 and November 27, 2018; accepted December 21, 2018. Date of publication January 1, 2019; date of current version February 22, 2019. This work was supported by the Materials and Parts Technology R&D Program funded by the Korean Ministry of Trade, Industry and Energy under Project 10065666. *(Corresponding author: Woo-Young Choi.)*

M.-H. Kim and W.-Y. Choi are with the Department of Electrical and Electronic Engineering, Yonsei University, Seoul 120-749, South Korea (e-mail: teramhkim@gmail.com; wchoi@yonsei.ac.kr).

L. Zimmermann is with the IHP, Frankfurt (Oder) 15236, Germany (e-mail: lzimmermann@ihp-microelectronics.com).

Color versions of one or more of the figures in this paper are available online at http://ieeexplore.ieee.org.

Digital Object Identifier 10.1109/JLT.2018.2889899

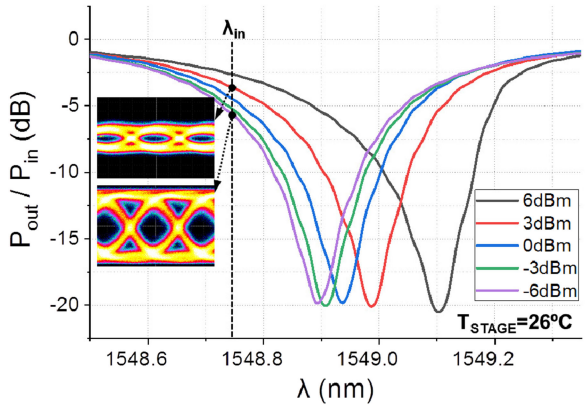

Fig. 2. Normalized transmission spectra of sample Si MRM at five different input optical powers and eye diagrams at powers of 9-dB difference.

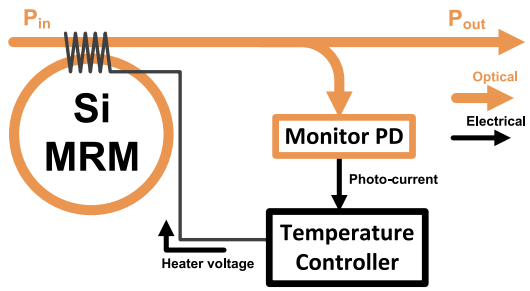

Fig. 3. Conceptual scheme of temperature controller for Si MRM.

10-μm ring radius, 2×10^{18} cm^{-3} doping for p-region, and 3×10^{18} cm^{-3} doping for n-region is placed on a temperature-controlled stage. Fig. 1(b) shows the sample device with its cross-sectional diagram. This Si MRM device is used for all the measurement results reported in this paper.

Furthermore, the Si MRM suffers from self-heating [3]. Fig. 2 shows the measured transmission characteristics with five different input optical powers while the stage temperature (T_{STAGE}) is fixed at 26 °C. With the larger input optical power, there is a larger amount of absorption of input light in the ring waveguide especially around the resonance wavelength causing higher temperature for the Si MRM, resulting in the larger resonance wavelength. As can be seen in the figure, this resonance wavelength shift produces dramatically different eye diagrams for the same device even when the stage temperature remains the same.

With above-mentioned thermal sensitivity problems, it is clear that for any practical application of the Si MRM a technique is required with which the resonance wavelength can be precisely controlled at the desired value regardless of the temperature or the input optical power. Fig. 3 shows the often-used scheme in which a temperature controller (TC) takes signals from a monitor photodetector (PD) and determine the optimal level of the signals supplied to the on-chip heater placed near the device so that it produces the optimal modulation performance for the given input light wavelength and power.

In this paper, we demonstrate a new type of TC that successfully performs the above-explained task. In particular, our TC is realized in the Si integrated circuit (IC), which should be an absolute must for any practical future inter-chip and intra-chip optical interconnect applications

This paper is organized as follows. In Section II, after a brief review of previously reported modulator TCs, we give details of our TC structure and its control algorithm. In Section III, we present experimental demonstration of our TC IC. Section IV concludes this paper.

II. Temperature Controller

There are several different types of controllers for optical modulators. In order to stabilize the bias voltage of the MZM, a slow pilot tone can be added to the bias voltage and the resulting ratio of the first- and second-order signals from the modulator output can be used as feedback for obtaining the optimal bias voltage [4]. By slowly dithering the MZM bias and coherently detecting 3×3 optical coupler outputs, the MZM bias can be automatically controlled for various modulation formats [5]. Error signals produced by mixing low-frequency dithering and monitored output signals can be used for locking the Si MRM at the optimal temperature producing the maximum optical modulation amplitude (OMA) [6]. However, these techniques require very low-frequency dithering signals typically in a few kHz range so that they do not interfere with modulator performance. Processing these low-frequency signals can be a serious problem for IC implementation since the required capacitor sizes can be very large.

There are others techniques that do not require low-frequency dithering. Directly monitoring of the MZM OMA can be achieved by processing high-speed data but it consumes a large amount of power [7]. The average optical output power can be monitored to determine the MZM bias producing the optimal OMA [8], but this technique is not suitable for the Si MRM application as it cannot determine the optimal condition when the input optical power changes.

There are several reports in which OMA monitoring is used for the Si MRM [9]–[11]. In [9], the average output power of the Si MRM is used in a closed-loop feedback with a predetermined offset so that its OMA is maximized, but the amount of detuning has to be independently determined. In [10], a bit-statistical algorithm based on non-DC-balanced data is used for optimizing OMA, but if the input optical power changes from the level used during the initial locking process its optimal performance may not be guaranteed. Direct OMA monitoring from high-speed sampling of four consecutive zeros-or-ones from monitored optical signals with data-slope quantization [11] is also used to determine the maximum OMA, but their accuracy is not guaranteed for short run-length data.

Our new TC IC for a Si MRM can alleviate above-mentioned problems. Fig. 4 shows the block diagram of our TC IC having three functional blocks: OMA monitor, control unit, and heater driver. The OMA monitor takes monitor-PD output currents, converts them into voltages with a trans-impedance amplifier (TIA). The TIA output is delivered after high-pass filtering to a power detector which produces V_{OMA} representing the modulator output OMA. The inset graph in Fig. 4 shows the simulated V_{OMA} dependence on the photo-current peak-to-peak values

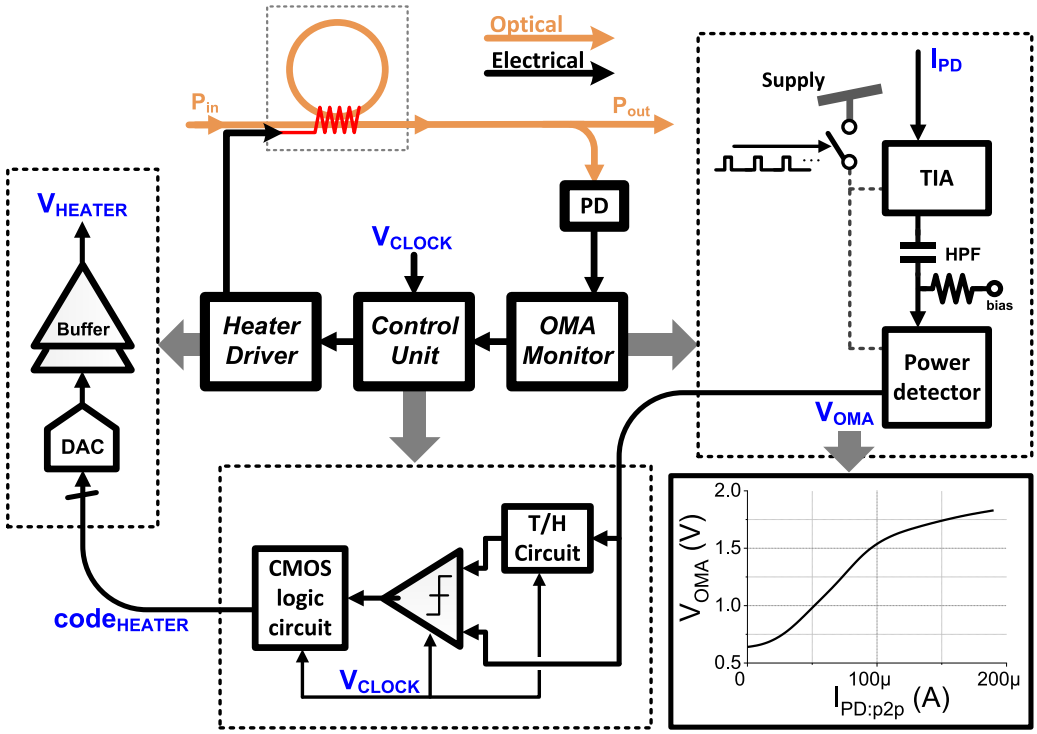

Fig. 4. Detailed block diagram of our temperature controller with optical setup.

($I_{PD:p2p}$) when the Si MRM is modulated with 25-Gb/s PRBS 2^7-1. This simulation is done in Verilog-A with the equivalent circuit models for Si MRM [12] and PD [13]. The control unit consists of track-and-hold (T/H) circuit, comparator, and synthesized CMOS logic circuits, which are synchronized with a clock signal supplied externally (V_{CLOCK}). This block carries out the control algorithm of searching and maintaining the maximum OMA value. The heater driver converts the digital code ($code_{HEATER}$) provided by the control unit into an analog signal (V_{HEATER}) by digital-to-analog converter (DAC) and buffer. The final voltage is delivered to the on-chip MRM heater.

When the TC IC is turned on, it begins searching of V_{HEATER} that produces the maximum V_{OMA} by scanning $code_{HEATER}$ with the pre-determined range and step, determination of which requires prior characterization of the target device. For each value of $code_{HEATER}$, V_{OMA} is measured and compared with its previous value using the T/H circuit and the comparator. If the present V_{OMA} is larger than the previous one, the present $code_{HEATER}$ is stored in a register as the maximum value ($code_{MAX}$). If not, the previous $code_{MAX}$ is maintained. From this searching step, our TC IC finally selects the last found optimal. In other words, it selects the shorter wavelength side optimal of the resonance since we find experimentally that the Si MRM operation is more stable here than in the longer wavelength side even if the resulting OMAs are the same.

After the searching step is over, the on-chip controller starts the maintaining step using $code_{MAX}$ as $code_{HEATER}$ and tries to maintain the optimal condition around this $code_{HEATER}$ value. In the maintaining step, the control unit counts up $code_{HEATER}$ by 1-bit and compare the resulting V_{OMA} value with the previous one. If the present value is larger than the previous one, the control unit counts up $code_{HEATER}$ by additional 1 bit. If not, the control unit reverses the counting in $code_{HEATER}$ and repeats the process. By this simple algorithm, $code_{HEATER}$ can continue to provide V_{HEATER} that produces the largest V_{OMA}, or the optimal Si MRM OMA. In addition, in order to save power consumption, the control unit does not continuously perform this maintaining process but periodically turns off the power of the OMA monitor block when unnecessary. The duration and frequency of this maintaining process can be easily programmed into the control unit as desired. Fig. 5 shows the flowchart for above-explained algorithm.

Details of IC implementation are as follows. The TIA in Fig. 6 is designed with a regulated cascode structure [14]. The HPF is designed so that it has the cut-off frequency of 2-MHz, which causes 1.6% DC-droop for 31 consecutive bit sequence. The HPF consists of 4-pF metal-insulator-metal capacitor and 20-kΩ resistor, both of which have about 0.012-mm^2 area. The power detector in Fig. 6 is designed with a common-emitter amplifier typically used for the RF amplitude monitoring application [15]. The supply voltage of TIA and the power detector is power-connected with a regulator controlled from the control unit. The T/H circuit uses a structure with charge-offset cancellation [16]. The comparator uses a negative edge-triggered sense-amplifier based D flip-flop, which is widely used for high-sensitivity applications. The DAC is designed with R-2R ladder structure. The buffer within the heater driver is designed with a regulator-type unit-gain buffer which consumes about 180 μW. Our sample Si MRM has the integrated on-chip heater realized with p-type Si resistor located near the directional coupler within the MRM as shown in Fig. 1(b). It has the measured resistance of 1.6-kΩ and has efficiency of 68-pm resonance shift per mW.

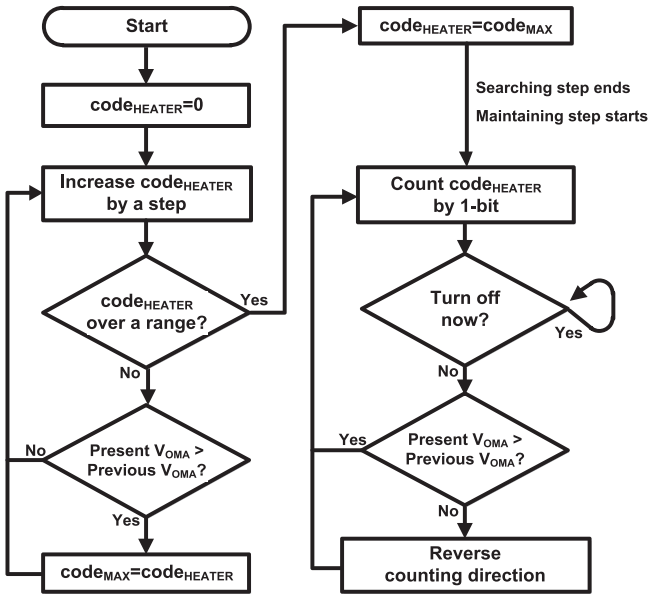

Fig. 5. Flowchart for two-step temperature control algorithm.

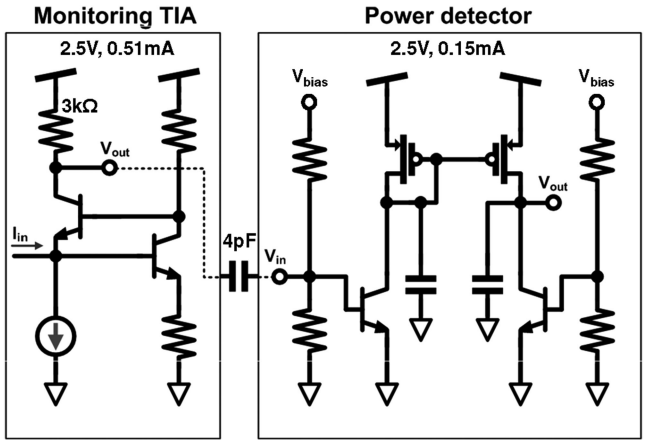

Fig. 6. Detailed schematics of TIA and power detector in OMA monitor.

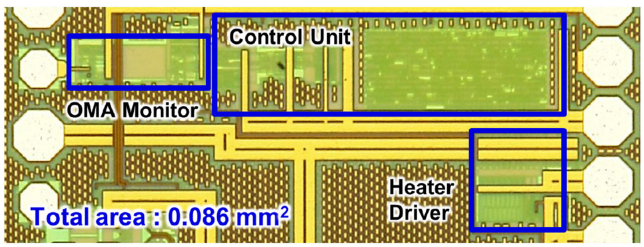

Fig. 7. Microphotograph of the fabricated temperature controller IC.

The CMOS logic circuits in the control unit are implemented with the standard CMOS digital cell library. It has 380 gates including 69 registers.

Fig. 7 shows the fabricated TC IC chip realized with IHP's 0.25-μm BiCMOS technology. The IC is implemented in this technology because our goal is realization of monolithic integration of Si MRMs that we have demonstrated (for example, [17]) with the TC IC based on IHP's Photonic BiCMOS technology

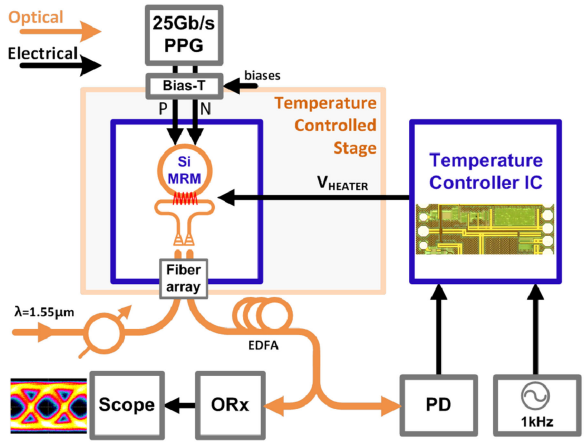

Fig. 8. Measurement setup for temperature controller IC test.

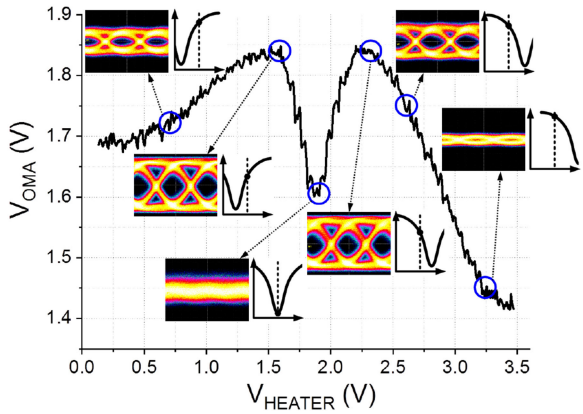

Fig. 9. Measured V_{OMA} as a function of V_{HEATER} during the searching step, measured 25-Gb/s PRBS 2^7-1 eye diagrams at six different conditions, and their locations of relative Si MRM resonance wavelength.

[18], which allows on-chip integration of high-performance Si photonic devices along with 0.25-μm BiCMOS technology. The chip area is approximately 0.086-mm^2. In this implementation, 4-bits are used for the step of $code_{HEATER}$ scanning, 8-bits for DAC, 1-kHz for V_{CLOCK}, 1-sec for the turn-off period, and 1:7 for its on-and-off ratio. With these, it takes 64-ms for the searching step and the maintaining step consumes 3.91-mW excluding the heater driver, which consumes 3-mW at 2.2 V of V_{HEATER}.

III. Measurements

In order to demonstrate the operation of our TC IC, the modulation characteristics of the sample Si MRM are measured with the TC IC in the experiment set-up shown in Fig. 8. 1549.16-nm light is coupled into a Si MRM device placed on a temperature-controlled chip stage through a grating coupler, the modulated output light is coupled out with another grating coupler. Each grating coupler has about 4.5 dB coupling loss. The modulator has FSR of 5 nm, quality factor of about 3400. It is modulated with 4-V_{p2p} 25-Gb/s PRBS 2^7-1 and $2^{31}-1$ data supplied by a pulse-pattern generator. When the Si MRM has the maximum OMA, there is 6 dB insertion loss. This results in the total insertion loss of about 15 dB including two grating couplers. In

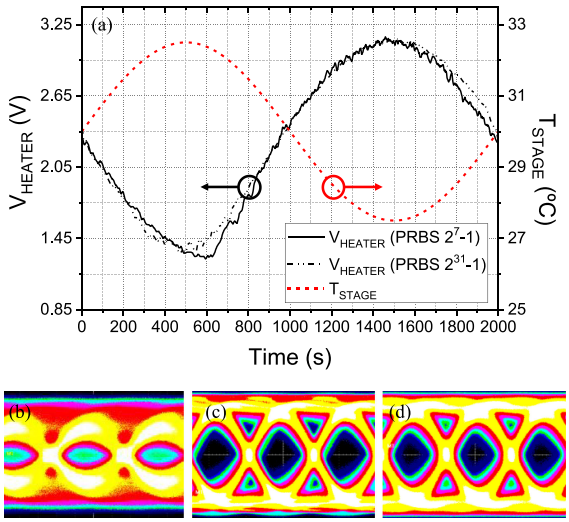

Fig. 10. (a) Measured transient response of V_{HEATER} in the maintaining step when T_{STAGE} is intentionally changed in a sinusoidal pattern around 30 °C with ±2.5 °C maximum fluctuation at 0.5-mHz frequency, and simultaneously measured 25-Gb/s eye diagrams accumulated for 2000 seconds (b) without TC IC, (c) with TC IC for PRBS 2^7-1, and (d) with TC IC for PRBS $2^{31}-1$.

this condition, our device has ER of about 2.57 dB. The optical powers given for various experiments in the paper are those introduced to the MRM device after the input grating coupler.

The output light is delivered to an external monitor PD through an EDFA used for compensating the losses such as 9-dB from two grating couplers. An external monitor PD should be unnecessary when the Si MRM is integrated with a monitor Ge PD along with couplers. In this feasibility demonstration, a commercial InGaAs PD is used as the monitor PD. The PD output is delivered to our TC IC placed on a FR4 board.

Fig. 9 shows the measured V_{OMA} as a function of V_{HEATER} during the searching step in which V_{HEATER} increases from the ground to 3.6-V. Also shown are measured eye diagrams for several different V_{HEATER} values. For each eye diagram, the location of the input wavelength relative to the MRM resonance peak at that V_{HEATER} is shown schematically. As V_{HEATER} increases, the resonance wavelength shifts to the larger value. As can be seen in the figure, two V_{HEATER} values of about 1.6-V and 2.3-V provide the largest V_{OMA} as well as the best eye diagrams. The control unit selects 2.3-V as V_{HEATER} producing the optimal V_{OMA} as the control unit keeps the last found maximum value and uses it as the starting value for the maintaining step. For this measurement, T_{STAGE} is maintained at 30 °C and the input optical power is 0-dBm.

Fig. 10(a) shows the measured V_{HEATER} values in the maintaining step when T_{STAGE} is intentionally changed in a sinusoidal pattern around 30 °C with ±2.5 °C maximum fluctuation and 0.5-mHz frequency. The input optical power is maintained to 0-dBm. It is clearly shown that our TC IC automatically changes V_{HEATER} so that the optimal V_{OMA} can be maintained. Fig. 10(b) shows the accumulated eye diagrams for 2000 seconds without our TC IC operation, Fig. 10(c) with TC IC for PRBS 2^7-1, and (d) for PRBS $2^{31}-1$. Fig. 11(a) and (b) show the same measurement results as in Fig. 10 except that T_{STAGE}

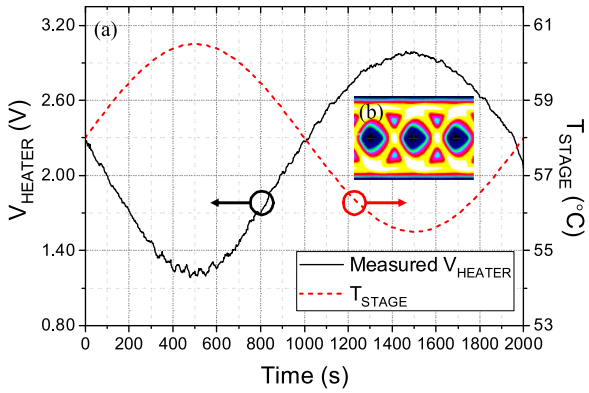

Fig. 11. (a) Measured transient response of V_{HEATER} in the maintaining step when T_{STAGE} is intentionally changed in a sinusoidal pattern around 57.5 °C with ±2.5 °C maximum fluctuation at 0.5-mHz frequency, and (b) simultaneously measured 25-Gb/s PRBS $2^{31}-1$ eye diagram accumulated for 2000 seconds with our TC IC.

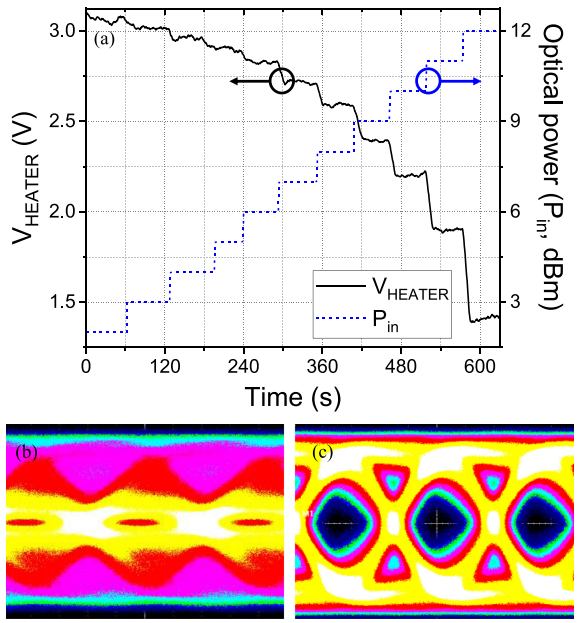

Fig. 12. (a) Measured transient response of V_{HEATER} in the maintaining step when input optical power is intentionally changed in a step of about 1-dBm for duration of 1 minute and simultaneously measured 25-Gb/s PRBS $2^{31}-1$ eye diagrams accumulated for 630 seconds (b) without and (c) with our TC IC.

fluctuates around 57.5 °C with ±2.5 °C, for which the required input wavelength shifts to 1547.81-nm. Clearly, with our TC IC, the optimal modulation characteristics are well maintained even when T_{STAGE} fluctuates. With the present TC IC, it can compensate T_{STAGE} fluctuation of up to about 6.5 °C, which is less than the entire FSR. This is due to the low heater efficiency and the limited maximum value of V_{HEATER} that our TC IC can produce. With additional circuit techniques such as DC-DC converter [19] along with more efficient on-chip heaters [20], [21], the tuning range can be significantly extended. If it becomes possible to cover the entire FSR with these improvements, our TC algorithm can be modified so that the initial scan range does not have to be pre-determined.

TABLE I
STATE-OF-THE-ART COMPARISON

	[10]	[11]	This work
Scheme	Non-DC-balanced bit-statistics	OMA monitor w/ slope quantization	OMA monitor w/ power detector & two-step approach
Process	45nm CMOS	130nm SOI + 40nm CMOS	0.25μm BiCMOS
Integration	Monolithic	Flip-chip	External
Demo. data-rate	5 Gb/s	2 Gb/s	25 Gb/s
Temperature fluctuation	Few tens of mHz*	5 kHz	0.5 mHz
Heater efficiency	1.25 nm/mW	150 pm/mW	68 pm/mW
Resonance wavelength tuning range	2.5 nm	5 nm	0.55 nm
Power**	0.72 mW	2.9 mW	3.91 mW
Energy/bit	0.144 pJ/bit	1.45 pJ/bit	0.156 pJ/bit
Area	N/A	0.009mm^2	0.086mm^2

* Estimated value from results
** Excluding heater power dissipation

Fig. 12(a) shows how V_{HEATER} changes in the maintaining step when the input optical power to Si MRM increases from 2.8-dBm to 11.8-dBm in a step of about 1-dBm for duration of 1-min. For this measurement, T_{STAGE} is maintained at 30 °C. Once again, our TC IC changes V_{HEATER} accordingly so the optimal V_{OMA} can be maintained. Fig. 12(b) and (c) show the accumulated eye diagrams for 630 seconds without and with our TC IC operation. Once again, with our TC IC, the optimal modulation characteristics are well maintained despite input optical power fluctuation.

IV. CONCLUSION

A new temperature controller IC for the Si MRM is demonstrated. Our TC IC directly monitors the OMA from the Si MRM output and automatically searches and maintains the optimal heater voltage in a simple and low-power-consuming two-step approach. A prototype IC chip realized in 0.25-μm BiCMOS technology can successfully provide the temperature control for 25-Gb/s modulation for a 1550-nm Si MRM when the chip stage temperature or the input optical power changes.

ACKNOWLEDGMENT

The authors are thankful to IC Design Education Center (IDEC) for EDA tool supports.

REFERENCES

[1] M. Haurylau *et al.*, "On-chip optical interconnect roadmap: Challenges and critical directions," *IEEE J. Sel. Topics Quantum Electron.*, vol. 12, no. 6, pp. 1699–1705, Nov./Dec. 2006.
[2] W. Bogaerts *et al.*, "Silicon microring resonators," *Laser Photon. Rev.*, vol. 6, no. 1, pp. 47–73, 2012.
[3] M. J. Shin, Y. Ban, B. M. Yu, J. Rhim, L. Zimmermann, and W. Y. Choi, "Parametric characterization of self-heating in depletion-type Si microring modulators," *IEEE J. Sel. Topics Quantum Electron.*, vol. 22, no. 6, pp. 116–122, Nov./Dec. 2016.
[4] L. L. Wang and T. Kowalcyzk, "A versatile bias control technique for any-point locking in lithium niobate Mach–Zehnder modulators," *J. Lightw. Technol.*, vol. 28, no. 11, pp. 1703–1706, Jun. 1, 2010.
[5] X. Zhu, Z. Zheng, C. Zhang, L. Zhu, Z. Tao, and Z. Chen, "Coherent detection-based automatic bias control of Mach–Zehnder modulators for various modulation formats," *J. Lightw. Technol.*, vol. 32, no. 14, pp. 2502–2509, Jul. 15, 2014.
[6] K. Padmaraju, D. F. Logan, T. Shiraishi, J. J. Ackert, A. P. Knights, and K. Bergman, "Wavelength locking and thermally stabilizing microring resonators using dithering signals," *J. Lightw. Technol.*, vol. 32, no. 3, pp. 505–512, Feb. 1, 2014.
[7] M.-H. Kim, H.-Y. Jung, L. Zimmermann, and W.-Y. Choi, "An integrated Mach-Zehnder modulator bias controller based on eye-amplitude monitoring," *Proc. SPIE*, vol. 9751, Mar. 3, 2016, Art. no. 97510X.
[8] M.-H. Kim, B.-M. Yu, and W.-Y. Choi, "A Mach-Zehnder modulator bias controller based on OMA and average power monitoring," *IEEE Photon. Technol. Lett.*, vol. 29, no. 23, pp. 2043–2046, Dec. 2017.
[9] H. Li *et al.*, "A 25 Gb/s, 4.4 V-swing, AC-coupled ring modulator-based WDM transmitter with wavelength stabilization in 65 nm CMOS," *IEEE J. Solid-State Circuits*, vol. 50, no. 12, pp. 3145–3159, Dec. 2015.
[10] C. Sun *et al.*, "A 45 nm CMOS-SOI monolithic photonics platform with bit-statistics-based resonant microring thermal tuning," *IEEE J. Solid-State Circuits*, vol. 51, no. 4, pp. 893–907, Apr. 2016.
[11] S. Agarwal, M. Ingels, M. Pantouvaki, M. Steyaert, P. Absil, and J. Van Campenhout, "Wavelength locking of a Si ring modulator using an integrated drop-port OMA monitoring circuit," *IEEE J. Solid-State Circuits*, vol. 51, no. 10, pp. 2328–2344, Oct. 2016.
[12] M. Shin *et al.*, "A linear equivalent circuit model for depletion-type silicon microring modulators," *IEEE Trans. Electron Devices*, vol. 64, no. 3, pp. 1140–1145, Mar. 2017.
[13] J.-M. Lee, M. Kim, and W.-Y. Choi, "Series resistance influence on performance of waveguide-type germanium photodetectors on silicon," *Chin. Opt. Lett.*, vol. 15, 2017, Art. no. 100401.
[14] H. Y. Jung, J. M. Lee, and W. Y. Choi, "A high-speed CMOS integrated optical receiver with an under-damped TIA," in *Proc. IEEE Photon. Conf.*, Reston, VA, USA, 2015, pp. 347–350.
[15] A. S. Bakhtiar, M. S. Jalali, and S. Mirabbasi, "A high-efficiency CMOS rectifier for low-power RFID tags," in *Proc. IEEE Int. Conf. RFID*, Orlando, FL, USA, 2010, pp. 83–88.
[16] C. Eichenberger and W. Guggenbuhl, "Dummy transistor compensation of analog MOS switches," *IEEE J. Solid-State Circuits*, vol. 24, no. 4, pp. 1143–1146, Aug. 1989.
[17] M. Kim *et al.*, "A large-signal equivalent circuit for depletion-type silicon ring modulators," in *Proc. Opt. Fiber Commun. Conf. Expo.*, San Diego, CA, USA, 2018, Paper Th2A.13.
[18] L. Zimmermann *et al.*, "BiCMOS silicon photonics platform," in *Proc. Opt. Fiber Commun. Conf.*, 2015, Paper Th4E.5.
[19] J.-T. Wu and K.-L. Chang, "MOS charge pumps for low-voltage operation," *IEEE J. Solid-State Circuits*, vol. 33, no. 4, pp. 592–597, Apr. 1998.
[20] J. Sun *et al.*, "A 128 Gb/s PAM4 silicon microring modulator," in *Proc. Opt. Fiber Commun. Conf. Expo.*, San Diego, CA, USA, 2018, Paper Th4A.7.
[21] N. Sherwood-Droz *et al.*, "Optical 4×4 hitless silicon router for optical networks-on-chip (NoC): Erratum," *Opt. Express*, vol. 16, no. 23, pp. 19395–19395, 2008.

Min-Hyeong Kim (S'00) received the B.S. degree in electrical and electronic engineering in 2011 from Yonsei University, Seoul, South Korea, where he is currently working toward the Ph.D. degree. His research interests are Si-based electronic–photonic IC design and high-speed interface circuit design in CMOS or photonic BiCMOS technology.

Lars Zimmermann received degrees from Friedrich Schiller University, Jena, Germany, and Technische Universität Delft, Delft, The Netherlands, and the Ph.D. degree in electrical engineering from Katholieke Universiteit Leuven, Leuven, Belgium, for his work on near-infrared sensor arrays that he conducted at IMEC. In 2004, he joined the Technische Universität Berlin, Berlin, Germany, where he worked on integrated optics and hybrid integration. After joining IHP, Frankfurt (Oder), Germany, in 2008, he is currently a Team Leader of Silicon Photonics Technologies. He is also with the Technische Universität Berlin, coordinating the cooperation with IHP in the field of Si photonics.

Woo-Young Choi (M'92) received the B.S., M.S., and Ph.D. degrees in electrical engineering and computer science from the Massachusetts Institute of Technology, Cambridge, MA, USA, in 1986, 1988, and 1994, respectively. His doctoral dissertation concerned the investigation of molecular-beam epitaxy-grown InGaAlAs laser diodes for fiber-optic applications. From 1994 to 1995, he was a Postdoctoral Research Fellow with the NTT Opto-Electronics Laboratories, where he worked on femtosecond all-optical switching devices based on low-temperature grown InGaAlAs quantum wells. In 1995, he joined the Department of Electrical and Electronic Engineering, Yonsei University, Seoul, South Korea, where he is currently a Professor. His research interests are in the area of high-speed circuits and systems that include high-speed optoelectronics, high-speed electronic circuits, and silicon photonics.